

Distributed Construction of the Critical Geometric Graph in Dense Wireless Sensor Networks

Srivathsa Acharya*, Anurag Kumar*, Vijay Dewangan*, Navneet Sankara†,
Malati Hegde*, and S. V. R. Anand*

*Department of Electrical Communication Engineering, Indian Institute of Science, Bangalore, India
Email: srivatsa.acharya@gmail.com, anurag@ece.iisc.ernet.in, vijay.dewangan@gmail.com

†Department of Electrical Engineering, Indian Institute of Technology, Madras, India; Email: navsan@gmail.com

Abstract

Wireless sensor networks are often modeled in terms of a dense deployment of smart sensor nodes in a two-dimensional region. Given a node deployment, the *critical geometric graph (CGG)* over these locations (i.e., the connected *geometric graph (GG)* with the smallest radius) is a useful structure since it provides the most accurate proportionality between hop-count and Euclidean distance. Hence, it can be used for GPS-free node localisation as well as minimum distance packet forwarding. It is also known to be asymptotically optimal for network transport capacity and power efficiency. In this context, we propose DISCRIT, a distributed and asynchronous algorithm for obtaining an approximation of the CGG on the node locations. The algorithm does not require the knowledge of node locations or internode distances, nor does it require pair-wise RSSI (Received Signal Strength Indication) measurements to be made. Instead, the algorithm makes use of successful Hello receipt counts (obtained during a Hello-protocol-based neighbour discovery process) as edge weights, along with a simple distributed min-max computation algorithm.

In this paper, we first provide the theory for justifying the use of the above edge weights. Then we provide extensive simulation results to demonstrate the efficacy of DISCRIT in obtaining an approximation of the CGG. Finally, we show how the CGG obtained from DISCRIT performs when used in certain network self-organisation algorithms.

I. INTRODUCTION

In a wireless sensor network, the smart sensor nodes (often called *nodes*) are embedded in some space, region or structure in order to make measurements and to draw inferences. In this paper, we are concerned with situations in which there is a dense deployment of nodes over a 2-dimensional region. We propose and study an algorithm, called DISCRIT, for the distributed construction of an approximation to the *critical geometric graph (CGG)* over the set of node locations.

Notation: We denote the region of deployment by $\mathcal{A} \in \mathbf{R}^2$. Given a set of n nodes $N = \{1, 2, \dots, n\}$ and the node location vector $\mathbf{V} = (V_1, V_2, \dots, V_n) \in \mathcal{A}^n$, the *geometric graph (GG)* of radius r , denoted by $\mathcal{G}(\mathbf{V}, r)$, is obtained by joining any two nodes within a distance of r . That is, the edge set E of $\mathcal{G}(\mathbf{V}, r)$ is given by $E = \{(i, j) \in N^2 : d_{i,j} \leq r\}$, where $d_{i,j}$ represents the Euclidean distance between nodes i and j . A sufficiently small r can cause the resulting GG to be disconnected. Thus, the smallest r on the given node locations at which the corresponding GG becomes connected is called the *critical radius*, denoted as

$r_{crit}(\mathbf{V})$. We will call the corresponding GG, $\mathcal{G}(\mathbf{V}, r_{crit}(\mathbf{V}))$, the critical geometric graph (CGG) on \mathbf{V} . When the node locations are implicit, we denote the critical radius as r_{crit} and the CGG as \mathcal{G}_{crit} .

Motivation for \mathcal{G}_{crit} : The following are some reasons why it would be useful to develop a distributed algorithm for obtaining the CGG on a given set of node locations.

- 1) In most applications of wireless sensor networks, it is important for the nodes to be aware of their own locations and distances to other nodes (in particular the network's fusion centers, or base stations). While accurate and low-power Global Positioning System (GPS) support is becoming available on motes, such an approach may not only be expensive and power hungry, but also, not workable for all applications, for example in large indoor areas or in mines. One approach for GPS-free distance estimation and node localisation is to overlay a geometric graph on the node locations. It can then be shown that the number of edges along the shortest path between an *anchor point* on the plane and a node is roughly proportional to the Euclidean distance between the point and the node, *the proportionality factor being the radius of the GG* (see [1]). The usual approach for obtaining a GG on the set of node locations (e.g., [2] and [3]) yields a radius equal to the radio-range of the nodes. Since the CGG is the connected geometric graph (on the given node locations) with the smallest radius, it provides the "finest scale" with which to measure distances using hop-counts on a GG on the nodes.
- 2) Further, we observe that, since hop-counts on the CGG provide a measure of Euclidean distance, these hop-counts can also be used in topology-free routing. For example, a node that has a smaller hop-count (on the CGG) to the base-station is also likely to be closer to the base-station, and hence can serve as a forwarding node in a topology-free routing algorithm (see [4]).
- 3) We also recall that, under the setup used by Gupta and Kumar [5], \mathcal{G}_{crit} turns out to be an asymptotically optimal topology for maximising the transport capacity of the network, and minimizing the network power consumption.

Remark: Note that while Point 3) above suggests the use of \mathcal{G}_{crit} itself as the communication topology, in Points 1) and 2) \mathcal{G}_{crit} is used only as a means for obtaining distance measurements on the region on which the nodes are deployed.

System assumptions: To obtain a distributed algorithm to approximate \mathcal{G}_{crit} , we make the following assumptions. We consider a *dense* node deployment, where the nodes are deployed in excess of the minimum requirement for connectivity and sensing coverage. For the purpose of developing the theory, we consider the *uniform i. i. d.* deployment where each node is placed randomly uniformly on the region \mathcal{A} , independent of the placement of the other nodes. However, simulation results are shown for the *randomised lattice* and *grid* deployments as well. In a randomised lattice deployment, the region \mathcal{A} is divided into n partitions of equal area called cells, and one node is placed randomly over each cell. The grid is a deterministic deployment where the nodes are placed in \sqrt{n} rows and \sqrt{n} columns on \mathcal{A} , with the rows and columns equally spaced.

The channel model includes path loss, and fading with additive Gaussian noise, where the fading process is assumed to be stationary in space and time with a common marginal distribution. The terrain is assumed to be flat, and the node transmission is assumed to be omnidirectional, so that the power radiated in all directions is equal.

Contributions: With the above assumptions, our contributions are the following. We develop DISCRIT (DIStributed CRITICAL geometric graph algorithm), a distributed algorithm for constructing an approximation to \mathcal{G}_{crit} . The algorithm is based on a result due to Penrose [6] which holds for uniform i. i. d. deployments, and states that as the number of nodes $n \rightarrow \infty$ the CGG becomes the same as the *farthest nearest neighbour geometric graph (FNNGG)*. Given the internode distances, the FNNGG can easily be constructed by a

distributed max-min computation, thus providing an approximation to the CGG, for large n . Since we do not know internode distances, we utilise a technique that provides us with a monotone *decreasing* function of the internode distances, thus permitting the use of a *distributed min-max computation* to obtain the FNNGG. Such a function is obtained by using Hello reception counts obtained during the Hello-protocol-based neighbour discovery (see [7]). The Hello transmissions can proceed completely asynchronously (e.g., via CSMA broadcasts), thus not requiring transmission synchronisation, as might be necessary in an RSSI-based approach. We show theoretically (using our assumptions, above) that the counts we obtain can serve as surrogates for the internode distances directly in the special case of isotropic antenna radiation patterns. Then we provide extensive simulation results to support this theory and our overall DISCRIT proposal.

Finally, we provide numerical evaluations of two applications of the approximate CGG obtained from DISCRIT:

- 1) Optimal forwarding hop distance determination, as per the theory provided by Ramaiyan et al. in [8]
- 2) Hop Count Ration based Localisation (HCRL) ([9]).

Related Literature: Narayanaswamy et al. [10] provide the COMPOW protocol for obtaining \mathcal{G}_{crit} . The idea here is to operate all nodes at the lowest common power level of available discrete power levels while ensuring connectivity in the network. As the communication range is an increasing function of the transmission power, the minimum common power results in the minimum range for connectivity, and thus yields \mathcal{G}_{crit} . However, COMPOW requires distance-vector routing to be done for each available discrete power level; switching between power levels requires synchronisation among the nodes. Unlike COMPOW, the proposed algorithm DISCRIT does not require multiple power levels and synchronisation between nodes. Also, DISCRIT needs to be run only once by the nodes to obtain \mathcal{G}_{crit} , unlike COMPOW where routing has to be done for each power level. The literature related to using hop-distance as a measure of inter-node distance is discussed later in Section IV.

Outline of the Paper: Section II gives the algorithm DISCRIT for obtaining an approximation to \mathcal{G}_{crit} along with the associated theory (II-D). Section III provides simulation results on the performance of DISCRIT for various deployments. The CGG based distance discretisation technique and its justification are provided in Section IV. Finally, as an application of distance discretisation using DISCRIT, we provide numerical results for (i) a self-organisation formulation (Section V), and (ii) an approach for approximate node localisation (Section VI). Section VII concludes the paper with future work.

II. THEORY AND THE ALGORITHM

In this section, we first arrive at an algorithm for \mathcal{G}_{crit} by making use of a result by Penrose [6]. The algorithm requires each node to know the distances to its neighbours. The distance-free distributed algorithm (DISCRIT) is then obtained by using link-weights obtained from a Hello-protocol-based neighbour discovery as distance-like information.

A. Degree-1 GG and Penrose's Theorem

Given node locations \mathbf{V} , let $r_1(\mathbf{V})$ be the smallest r such that the corresponding GG, $\mathcal{G}(\mathbf{V}, r)$ has no *isolated* node, i.e., $\mathcal{G}(\mathbf{V}, r)$ has the *degree*¹ of at least 1. It can be seen that $r_1(\mathbf{V})$ is precisely the maximum of the nearest node distances, i.e.,

¹The degree of a node in a graph is the number of its *adjacent* nodes. The degree of a graph is the minimum of its node degrees.

$$r_1(\mathbf{V}) = \max_{i \in N} \left\{ \min_{j \in N, j \neq i} \{d_{i,j}\} \right\} \quad (1)$$

We call the corresponding GG, $\mathcal{G}(\mathbf{V}, r_1(\mathbf{V}))$ as the *degree-1 GG*, and denote it by \mathcal{G}_1 and $r_1(\mathbf{V})$ by r_1 when the node locations are implicit.

Consider a uniform i. i. d. deployment of n nodes. Thus the random node location vector \mathbf{V} corresponds to the probability space $(\mathcal{A}^n, \mathcal{F}^n, \mathcal{P}^n)$ where \mathcal{P} is the uniform measure on \mathcal{A} , \mathcal{P}^n is the corresponding product measure, and \mathcal{F}^n is the Borel field in \mathcal{A}^n . Theorem 1 gives the relationship between \mathcal{G}_1 and \mathcal{G}_{crit} for uniform i. i. d. deployment.

Theorem 1 (Penrose [6]): Let $\rho_k(\mathbf{V})$ be the minimum r at which $\mathcal{G}(\mathbf{V}, r)$ is k -connected², and $\sigma_k(\mathbf{V})$ be the minimum r at which $\mathcal{G}(\mathbf{V}, r)$ has degree k . Then

$$\lim_{n \rightarrow \infty} \mathcal{P}^n \{ \mathbf{V} : \rho_k(\mathbf{V}) = \sigma_k(\mathbf{V}) \} = 1$$

■

Since $\rho_1(\mathbf{V}) = r_{crit}(\mathbf{V})$ and $\sigma_1(\mathbf{V}) = r_1(\mathbf{V})$, we have

Corollary 1: $\lim_{n \rightarrow \infty} \mathcal{P}^n \{ \mathbf{V} : r_{crit}(\mathbf{V}) = r_1(\mathbf{V}) \} = 1$

■

Thus, Corollary 1 indicates that, for a dense node deployment, \mathcal{G}_1 is identical to \mathcal{G}_{crit} w.h.p.³. Note that in general, a graph with no isolated nodes need not be connected. But the result above implies that, if the graph is a GG and the node deployment is uniform i. i. d. then just having no isolated nodes ensures connectivity w.h.p. We thus look for a distributed construction of \mathcal{G}_1 , as it is the same as \mathcal{G}_{crit} w.h.p.

Now, suppose each node i knows the distances $d_{i,j}$ to each of its neighbours j . Then a node would know its nearest-neighbour distance too. As r_1 is the maximum nearest-neighbour distance from (1), a *distributed maximum-finding algorithm* can be run by each node to obtain r_1 . One such distributed maximum-finding algorithm is described in Section II-B. Once r_1 is known, each node includes all nodes within a distance of r_1 as its *adjacent nodes*. This results in a GG of radius r_1 , which is \mathcal{G}_1 .

B. An Algorithm for \mathcal{G}_1 using Distance Information

Here, every node i maintains a *range* $r(i)$ and an *adjacent node list* $N(i)$ which get updated as the algorithm progresses. At any iteration, $N(i)$ is the set of nodes whose distances are less than range $r(i)$ from node i .

- 1) **Initialisation:** For every node, the range is initialised to its nearest neighbour distance, and the adjacent node list contains only the nearest neighbour(s) and itself. That is, for all $i \in N$,

$$r^{(0)}(i) = \min_{j \in N, j \neq i} \{d_{i,j}\} \quad \text{and} \quad N^{(0)}(i) = \{j \in N : d_{i,j} \leq r^{(0)}(i)\}$$

Set the iteration index $k = 0$

- 2) **Current range unicast:** Every node i informs its current range $r^{(k)}(i)$ to all its current *adjacent nodes*, i.e., the nodes in $N^{(k)}(i)$. Therefore, the node i also receives values of current ranges from some of the nodes which belong to the set $S^{(k)}(i) = \{j \in N : i \in N^{(k)}(j)\}$.
- 3) **Updating the Adjacent Node List:** Every node i then updates its current range $r^{(k+1)}(i)$ to the maximum of the ranges it received. The maximum finding includes the node's current range $r^{(k)}(i)$

²A graph is k -connected if there exist k independent paths between any two nodes.

³w.h.p. stands for "with high probability," i.e., "with probability $\rightarrow 1$ as $n \rightarrow \infty$ ".

also. The adjacent node list $N^{(k+1)}(i)$ is also updated accordingly as the set of nodes whose distances from i are within $r^{(k+1)}(i)$.

$$r^{(k+1)}(i) = \max\{r^{(k)}(j) : j \in S^{(k)}(i)\} \quad \text{and} \quad N^{(k+1)}(i) = \{j \in N : d_{ij} \leq r^{(k+1)}(i)\}$$

- 4) **Terminating condition:** The algorithm terminates if all the ranges in an iteration remain unchanged, i.e.,
IF $r^{(k+1)}(i) = r^{(k)}(i)$ for all $i \in N$, **Call** $r(i) = r^{(k)}(i)$ and $N(i) = N^{(k)}(i)$; **STOP**
ELSE **Set** $k := k + 1$; **go to Step 2.**
Note that this is a *centralised* terminating condition. A *distributed* terminating condition is discussed later.
- 5) **Obtaining the topology:** The graph resulting from the algorithm G_A is obtained by joining each node i to each node in its final adjacent node list $N(i)$. i.e., $G_A = (\mathbf{V}, E_A)$ where $E_A = \{(i, j) : i \in N, j \in N(i)\}$. ■

The convergence of the algorithm output to \mathcal{G}_1 is given in the following theorem.

Theorem 2: If \mathcal{G}_1 is connected, then the algorithm converges to \mathcal{G}_1 , i.e., $\mathcal{G}_A = \mathcal{G}_1$, in at most D iterations, where D is the *hop diameter* of \mathcal{G}_1 .

Proof: See Appendix A for the proof. ■

From Corollary 1, \mathcal{G}_1 is indeed connected with high probability, i.e., $\mathcal{G}_1 = \mathcal{G}_{crit}$ w.h.p. Thus from Theorem 2, the algorithm above converges to \mathcal{G}_{crit} w.h.p.

Remarks 2.1: One can construct deployments where the algorithm fails to give a connected graph. However, these cases happen only when \mathcal{G}_1 is not connected (for if \mathcal{G}_1 is connected then Theorem 2 holds); the probability of this, as discussed above, is very small for dense networks (probability $\rightarrow 0$ as $n \rightarrow \infty$).

Remarks 2.2: Gupta and Kumar [11] have shown that r_{crit} scales as $r(n) = \Theta(\sqrt{\frac{\log n}{n}})$ w.p.1 as $n \rightarrow \infty$. Hence the hop diameter of \mathcal{G}_{crit} scales as $\Theta(\frac{1}{r(n)}) = \Theta(\sqrt{\frac{n}{\log n}})$ w.h.p. Thus, the algorithm converges in $\Theta\left(\sqrt{\frac{n}{\log n}}\right)$ iterations w.h.p.

Remarks 2.3: Note that after updating its range $r^{(k)}(i)$ to $r^{(k+1)}(i)$, the node i needs to communicate its new range (i.e., execute Step 2) only if it is different from the earlier range. In such a case, there will be no communication when the terminating condition in Step 4 is met. Hence, a *distributed* terminating condition would be that, after informing its current range, each node waits for a certain *time-out* period, and locally decides to terminate the algorithm if it receives no communication from any node during this period.

1) *Extension to Monotone Functions of Distances:* Theorem 2 can be shown to hold even in the case where the distances $d_{i,j}$ in the algorithm are replaced by $f(d_{i,j})$, where f is **monotone increasing**. Thus, if we have a *distance-like* information (a monotone function of distance) known at each node about all its neighbours, then a *distance-free* distributed algorithm for \mathcal{G}_{crit} can be obtained. For this purpose, we consider the Hello-protocol-based neighbour discovery proposed by Karnik and Kumar [7], and use certain *link weights* obtained from the neighbour discovery as surrogates for distances. We assume that the antennas of all the motes have isotropic radiation patterns. Such radiation isotropy is a valid assumption for external “stick” antennas. The resulting distance-free algorithm, DISCRIT, is described in Section II-D. The Hello-protocol-based neighbour discovery is described next, along with a discussion of monotonicity of link weights under these conditions. Under antenna pattern anisotropy (e.g., on-board “patch” or “integrated circuit” antennas), however, these link weights are found not to be monotonic with distance. In related work (not reported here) we have

pursued an approach to collate the link weights from neighbouring nodes in order to obtain a monotonic function of distance.

C. Hello-Protocol-Based Neighbour Discovery

For the present discussion, we consider a slotted system. Note that this is *not* a necessary requirement. Indeed, the algorithm developed here easily applies to CSMA/CA scheduling. We have implemented the algorithm on a *Qualnet* simulator where IEEE 802.11b CSMA/CA is used, and *the results reported later in Section III are with the CSMA/CA*. In each slot, a node chooses to be either in the transmit mode with probability α , or in receive mode with probability $1 - \alpha$. Whenever in the transmit state, the node broadcasts a Hello packet where the Hello packet could simply be a packet containing the node *id*. Let $H_{i,j}$ represent the fading coefficient from i to j , with cumulative distribution $A(\cdot)$, which is assumed to be identical across all transmit-receive pairs (i, j) . To model if a Hello packet of a transmit node i has been successfully decoded by a receive node j , the *physical model* for communication can be used. That is, transmission from i to j in a slot is successful if the signal-to-interference-plus-noise ratio (SINR) of i at j is above a threshold β , i.e., if

$$SINR(i, j) = \frac{H_{i,j}P_t/d_{i,j}^\eta}{\sigma^2 + \sum_{k \in N, k \neq i} (H_{k,j}P_t/d_{k,j}^\eta)I_k} \geq \beta$$

where P_t is the node transmit power at a reference distance, η is the path loss exponent, and σ^2 is the noise variance. I_k is the indicator function of the event that the node k is simultaneously transmitting in the same slot, given that i is transmitting in the slot.

This process of broadcasting Hello packets is carried out for a large number of slots t . Let $C_{i,j}(t)$ be the count of Hellos of i received at j . Let $B_i(t)$ be the number of Hellos broadcast by i during this period. At the end of t slots, each receive node j calculates $\frac{C_{i,j}(t)}{B_i(t)}$ which is the fraction of Hellos of i decoded by j .

Let $p_{i,j}$ be the probability that i 's Hello is successfully received at j , under the broadcast setting described above. Thus $p_{i,j}$ is the probability that in the slot in which i is transmitting, j is in receive mode, and the SINR of i at j is greater than β , i.e.,

$$p_{i,j} = (1 - \alpha) \Pr \left(\frac{H_{i,j}P_t/d_{i,j}^\eta}{\sigma^2 + \sum_{k \in N, k \neq i} H_{k,j}P_t/d_{k,j}^\eta I_k} \geq \beta \right) \quad (2)$$

Since the system activity is independent from slot to slot, by the strong law of large numbers, we have, with probability one

$$\lim_{t \rightarrow \infty} \frac{C_{i,j}(t)}{B_i(t)} = p_{i,j} \quad (3)$$

The $p_{i,j}$ estimate thus obtained above is used by node j as the *receive link weight* of the link (i, j) . We now analyse the monotonicity of $p_{i,j}$ with $d_{i,j}$ for its applicability as distance-like information.

1) *Monotonicity of $p_{i,j}$ with $d_{i,j}$ Under Isotropic Conditions:* From Equation 2, we have

$$\begin{aligned}
p_{i,j} &= (1 - \alpha) \Pr \left\{ \frac{H_{i,j} P_t / d_{i,j}^\eta}{\sigma^2 + \sum_{k \in N} (H_{k,j} P_t / d_{k,j}^\eta)} I_k - H_{i,j} P_t / d_{i,j}^\eta \geq \beta \right\} \\
&= (1 - \alpha) \Pr \left\{ (1 + \beta) H_{i,j} P_t / d_{i,j}^\eta \geq \beta \left(\sigma^2 + \sum_{k \in N} (H_{k,j} P_t / d_{k,j}^\eta) I_k \right) \right\} \\
&= (1 - \alpha) \Pr \left\{ \mathcal{I}_j \leq \frac{(1 + \beta) H_{i,j} P_t}{\beta d_{i,j}^\eta} - \sigma^2 \right\}
\end{aligned}$$

where $\mathcal{I}_j := \sum_{k \in N} (H_{k,j} P_t / d_{k,j}^\eta) I_k$ is the random variable that represents the total power received at j .

For a large *spatially homogeneous* network, where the node density is constant over the entire region, the total power received at each node \mathcal{I}_j can be assumed to be identically distributed at all node locations, with common CDF $F(\cdot)$. This assumption will be shown to be valid (to a good approximation) for the interior nodes using simulations in III-A. Then, using $A(\cdot)$, the cumulative distribution function of $H_{i,j}$ (which is assumed to be identical across all (i, j)), the equation above becomes

$$p_{i,j} = (1 - \alpha) \int_0^\infty F \left(\frac{(1 + \beta) h P_t}{\beta d_{i,j}^\eta} - \sigma^2 \right) dA(h) \quad (4)$$

Since $F(\cdot)$ and $A(\cdot)$ are monotone increasing functions (as both are CDFs), it can be seen from Equation 4 above that $p_{i,j}$ is monotone decreasing with $d_{i,j}$. This allows us to replace $d_{i,j}$ in the previous algorithm (in Section II-B) by $-p_{i,j}$, to obtain a distance-free algorithm which is described next in Section II-D.

D. DISCRIT: DISTRibuted CRITICAL geometric graph algorithm

At the end of the Hello-protocol based neighbour discovery, each node i has link weights $p_{j,i}$ for each of its neighbours j . Every node i maintains a p -threshold $p(i)$ and an adjacent node list $N(i)$. At any iteration, $N(i)$ is the set of nodes j whose $p_{j,i}$ values are greater than or equal to p -threshold $p(i)$.

- 1) **Initialisation:** For every node i , the p -threshold $p^{(0)}(i)$ is initialised to the maximum link weight, and the adjacent node list $N^{(k)}(i)$ contains only the node(s) with the maximum weight. That is, for all $i \in N$,

$$p^{(0)}(i) = \max_j \{p_{j,i}\} \quad \text{and} \quad N^{(0)}(i) = \arg \max_j \{p_{j,i}\}$$

Set iteration index $k = 0$.

- 2) **p -threshold unicast:** Every node i informs its current p -threshold $p^{(k)}(i)$ to all its current *adjacent nodes*, i.e., nodes in $N^{(k)}(i)$. Thus, the node i also receives the p -thresholds $p^{(k)}(j)$ from some of its neighbours given by the set $S^{(k)}(i) = \{j : i \in N^{(k)}(j)\}$.
- 3) **Updating the Adjacent Node List:** The node then updates its p -threshold $p^{(k+1)}(i)$ to the minimum of the p -thresholds it received. The minimum finding includes the node's current p -threshold $p^{(k)}(i)$ also. The adjacent node list $N^{(k+1)}(i)$ is also updated accordingly as the set of nodes whose $p_{j,i}$ s are greater than the updated p -threshold $p^{(k+1)}(i)$. Let $t^{(k)}(i) = \min\{p^{(k)}(j) : j \in S^{(k)}(i)\}$, which is the smallest of the p -thresholds received by i . Then

$$p^{(k+1)}(i) = \min\{p^{(k)}(i), t^{(k)}(i)\} \quad \text{and} \quad N^{(k+1)}(i) = \{j : p_{j,i} \geq p^{(k+1)}(i)\}$$

- 4) **Terminating Condition:** The algorithm terminates if all the p -thresholds in an iteration remain unchanged, i.e.,

$$\text{IF } p^{(k+1)}(i) = p^{(k)}(i) \text{ for all } i \in N, \quad \text{Call } N(i) = N^{(k)}(i), \quad \text{STOP}$$

ELSE Set $k = k + 1$, go to **Step 2**.

The distributed terminating condition is as described for the algorithm based on distances, and can be used by the nodes to terminate locally.

- 5) **Making links bidirectional:** Let $S(i) = \{j : i \in N(j)\}$. Thus $S(i)$ represents the nodes having i as its adjacent node. The bidirectionality is achieved by updating the adjacent node list as $N(i) = N(i) \cup S(i)$. The graph resulting from the algorithm $\hat{\mathcal{G}}_1$ is then given by $\hat{\mathcal{G}}_1 = (\mathbf{V}, \hat{E}_1)$ where $\hat{E}_1 = \{(i, j) : i \in N, j \in N(i)\}$ ■

Remarks 2.4: Unlike distances $d_{i,j}, p_{i,j} \neq p_{j,i}$ in general. Therefore, the graph obtained after the terminating condition in Step 4 need not be bidirectional. Hence, additional edges are added to the graph in Step 5 to ensure bidirectionality.

Remarks 2.5: Note that for DISCRIT to be valid, we need *spatial homogeneity* for $p_{i,j}$ monotonicity as well as the Penrose's result (Corollary 1) to hold. While randomised lattice and grid deployments are spatially homogeneous, a uniform i.i.d. deployment, in general, can create *sparse* and *dense* node placements. However, as n is increased, uniform i. i. d. deployment is homogeneous w.h.p. in a sense described below. Further, Corollary 1 is known to be true for uniform i. i. d. deployment. We will use simulations to study the applicability to other deployments.

Given a uniform i. i. d. deployment \mathbf{V} , any $r > 0$, and any point x within the region \mathcal{A} , define *closed disc* of radius r around x , $D_r(x) := \{y \in \mathbf{R}^2 : \|y - x\| \leq r\}$. Let $N_r(x; \mathbf{V})$ be the number of nodes in $D_r(x)$, i.e., within a radius of r around x . Define the *interior* of \mathcal{A} as $\tilde{\mathcal{A}}(r) = \{x \in \mathcal{A} : D_r(x) \subset \mathcal{A}\}$. The following theorem gives the joint convergence of $N_r(x; \mathbf{V})$ for all $x \in \tilde{\mathcal{A}}(r)$.

Theorem 3: For any $\epsilon > 0$ however small,

$$\lim_{n \rightarrow \infty} \mathcal{P}^n \left\{ \mathbf{V} : \frac{n}{|\mathcal{A}|} (1 - \epsilon) \leq \frac{N_r(x; \mathbf{V})}{\pi r^2} \leq \frac{n}{|\mathcal{A}|} (1 + \epsilon) \text{ for every } x \in \tilde{\mathcal{A}}(r) \right\} = 1$$

Proof: See Appendix B ■

The result above implies that, for a uniform i. i. d. placement of nodes, the node density around every *interior* point, i.e., $\frac{N_r(x; \mathbf{V})}{\pi r^2}$, is arbitrarily close to the network density $\frac{n}{|\mathcal{A}|}$ w.h.p., thus implying the homogeneity of dense uniform i. i. d. deployments.

Remarks 2.6: For finite regions, even when the deployment is spatially homogeneous, there will be an **edge effect**. The received power at a periphery node is usually less compared to the receive power at the nodes in the interior, because of the difference in node density at the periphery and the centre of the region (non-homogeneity at the edges)⁴. This *edge effect* will distort the behaviour of DISCRIT, as will be seen in the simulation results in Section III. A remedy for *edge effect* is to extend the node deployment beyond the boundaries of the area of interest, so that the actual region of interest does not experience the edge effect.

III. DISCRIT:SIMULATION RESULTS

A. Power Distribution

In Section II-D, we assumed that the total power at a receiver node (Signal + Interference + Noise) is identically distributed at every receiver. When the number of nodes is sufficiently large, a receiver far away

⁴Note that even the homogeneity result in Theorem 3 is applicable at the *interior* of the region, and not at the edges.

from the edges sees almost the same concentration of nodes around it and hence experiences the same distribution of total received power. This is particularly so if the exponent for power loss with distance η is large, because only the nearby nodes can make a measurable difference to the power received. This also reduces the “edge effect” seen by the receivers close to the edges.

For a verification of this in simulation, two random deployments of nodes in a unit square were considered, one with 1000 nodes and the other with 5000 nodes. η is also varied from 2.0 to 4.0. In each case, a large number of time slots of the slotted-Aloha protocol were simulated in Matlab, where each node transmits with some probability α independent of all other nodes, and acts as a receiver otherwise. The nodes in the unit square are also divided into 5 concentric annular regions of nodes of equal width (of 0.1 units). The total power received at the nodes in each region was calculated and an empirical probability of occurrence of each value of power (upto a certain resolution) was calculated. The resulting empirical distribution of powers is shown in Figure 1.

We notice from Figure 1 that, for a given number of nodes (1000 or 5000), the assumption of the same received power distribution across nodes becomes better as the path loss exponent, η , increases, and as the nodes are taken farther away from the edge of the region. The assumption also works better for a larger node density. In fact, we see that for 5000 nodes, distributed independently and uniformly over the region, and $\eta = 4$, the approximation is excellent for nodes lying at points greater than 0.1 units from the boundary.

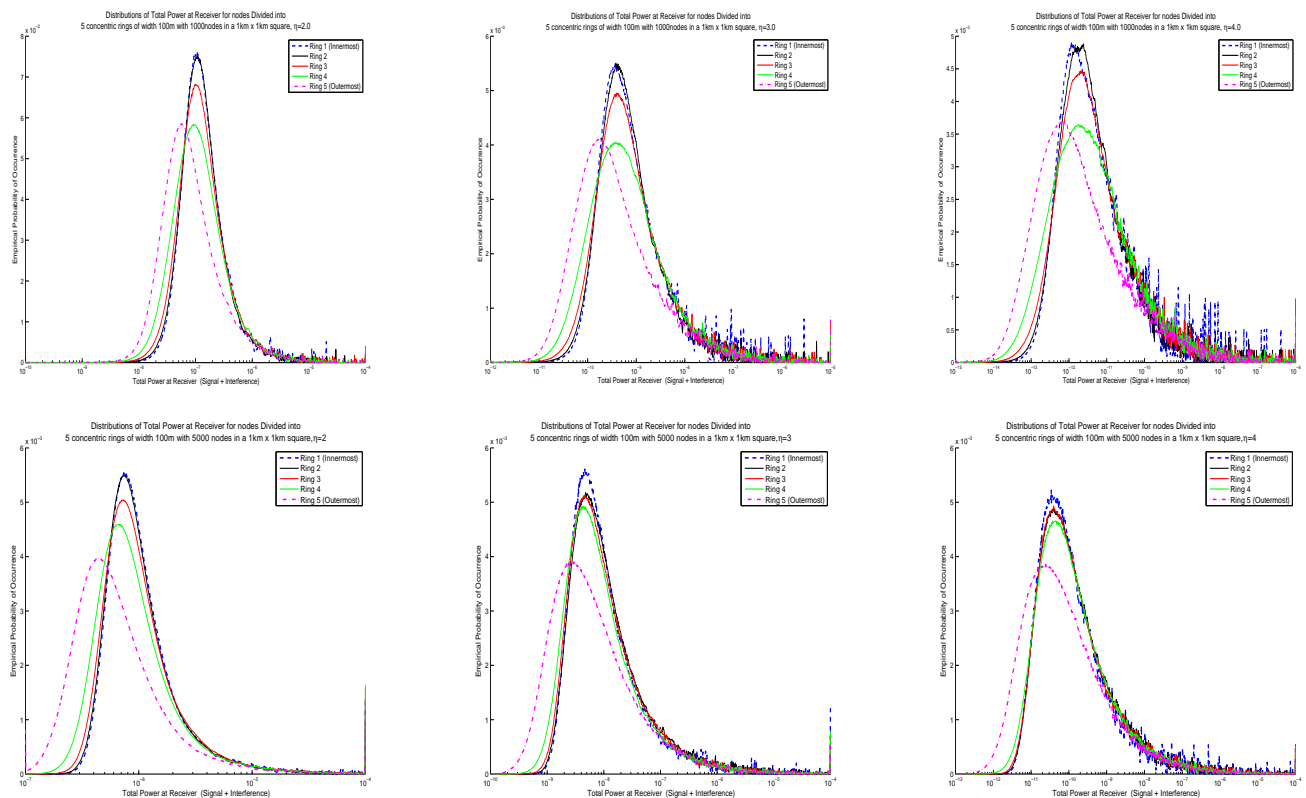


Fig. 1. Empirical histograms of total received power at nodes in 5 concentric annular regions in a 1 Km \times 1 Km region, with the nodes distributed independently and uniformly over the region. The top row corresponds to 1000 nodes, and the bottom row to 5000 nodes. The columns in this 2 \times 3 array of plots correspond successively to path loss exponents $\eta = 2, 3, 4$.

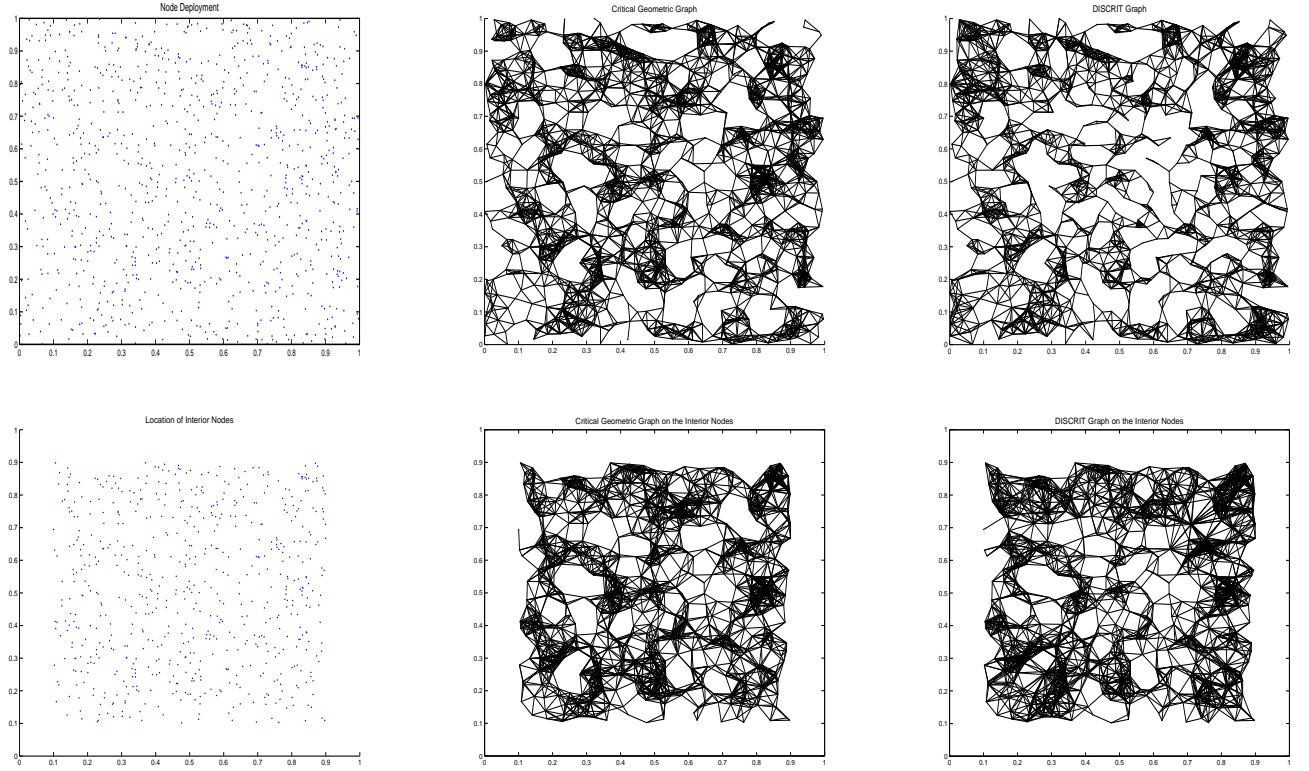


Fig. 2. Uniform i.i.d. deployment: Comparison of the critical geometric graph and the approximation provided by DISCRIT. The leftmost column of plots shows the node locations, the middle column the critical geometric graph, and the rightmost column the result obtained from DISCRIT. In the bottom row of plots the algorithm is run only on the “interior” nodes shown in the leftmost plot.

B. Performance of DISCRIT

Simulations were carried out in Matlab using both random and uniform (randomised lattice) deployments of 1000 nodes in a unit square region. In both cases, the DISCRIT algorithm was performed on the deployment under isotropic conditions and the results were compared with the respective Critical Geometric Graphs for the deployments.

Figure 2 provides results for uniform i.i.d. deployment. From a visual comparison of the actual CGG and the graph provided by DISCRIT we conclude that DISCRIT provide a graph with a similar visual structure, though with fewer links (we will evaluate this quantitatively below). In the light of the discussion about “edge effects” in Remarks 2.6, the nodes that were less than 0.1 units away from any edge of the unit square were removed and all the preceding analysis was performed on the interior node deployments, using the same link weights from Hello protocol for the entire deployment. The resulting DISCRIT output graph and CGG can be seen to be visually much closer to the actual CGG on the interior nodes. Similarly, Figure 3 provides the results from DISCRIT for the randomised lattice deployment.

1) *A quantitative measure of similarity between the CGG and output of DISCRIT:* We introduce a two-part measure to estimate the similarity between the approximate GG given by DISCRIT, $\hat{\mathcal{G}}_1$ and the true critical geometric graph, \mathcal{G}_{crit} or the FNNGG \mathcal{G}_1 . A geometric graph (GG) of radius r is defined by two criteria :

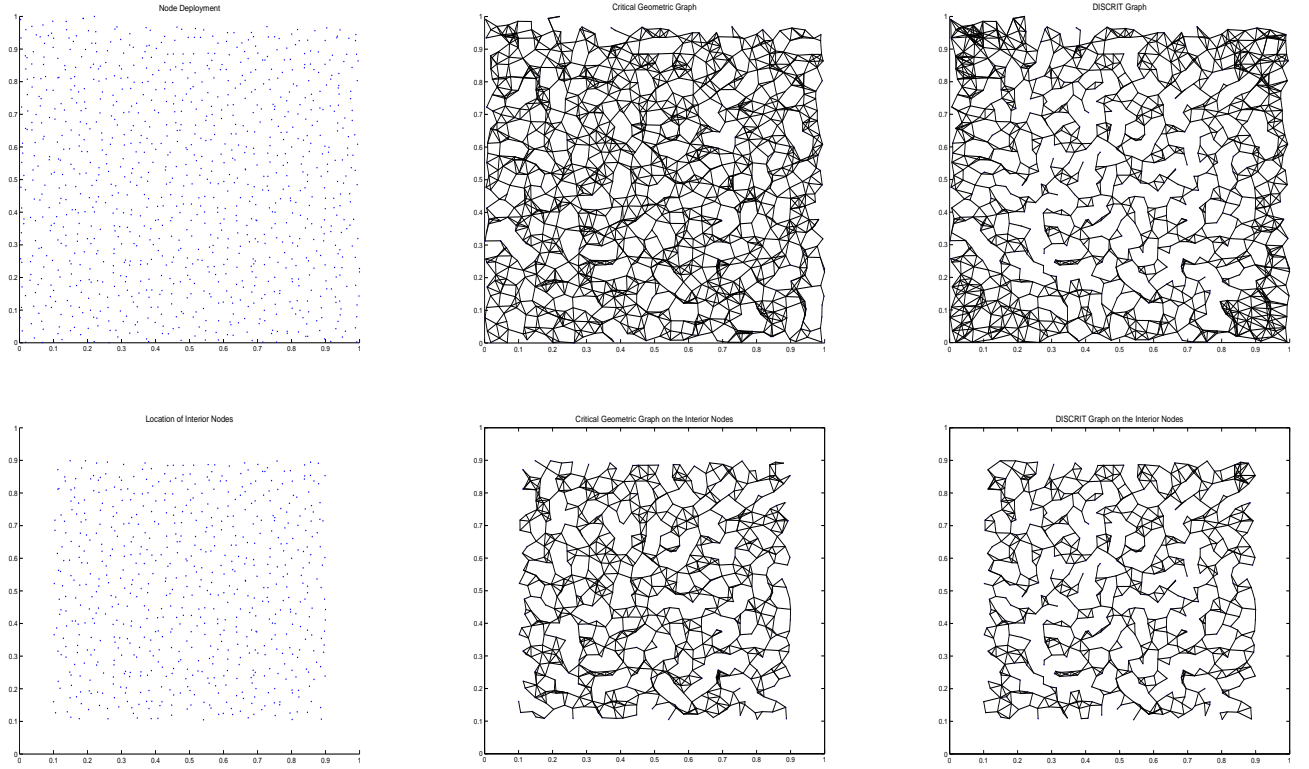


Fig. 3. Randomised lattice deployment: Comparison of the critical geometric graph and the approximation provided by DISCRIT. The leftmost column of plots shows the node locations, the middle column the critical geometric graph, and the rightmost column the result obtained from DISCRIT. In the bottom row of plots the algorithm is run only on the “interior” nodes shown in the leftmost plot.

- 1) No edges of length more than r should be present.
- 2) All edges of length at most r should be present.

Accordingly, we have defined the function $D(\cdot)$ on a pair of graphs G_1 and G_2 as $D(G_1, G_2) = \frac{|E_1 \cap E_2^c|}{|E_1|}$, where E_i is the edge set of graph G_i , for $i = 1, 2$. $D(\hat{G}_1, \mathcal{G}_{crit})$ is the fraction of edges of \hat{G}_1 that are longer than r_{crit} and $D(\mathcal{G}_{crit}, \hat{G}_1)$ is the fraction of edges shorter than r_{crit} that are missing in \hat{G}_1 . Ideally, both these quantities should be 0.

Simulation results shown in Table I show that the DISCRIT output is a very good approximation to the corresponding critical geometric graph and FNNGG, particularly when only the interior nodes are considered. Note that the exact degree-1 GG is in fact identical to the critical GG for the i.i.d. and grid deployments as well as for the interior nodes in the randomised lattice deployment. This shows that Penrose’s Corollary 1, though applicable only asymptotically, practically holds even for finite node densities.

Deployment	G_1	G_2	$D(G_1, G_2)$		$D(G_2, G_1)$	
			All Nodes	Interior Nodes	All Nodes	Interior Nodes
i.i.d	$\hat{\mathcal{G}}_1$	\mathcal{G}_{crit}	0.0610	0.1248	0.1656	0.0793
	\mathcal{G}_1	\mathcal{G}_1	0.0610	0.1248	0.1656	0.0793
Randomised Lattice	$\hat{\mathcal{G}}_1$	\mathcal{G}_{crit}	0.0834	0.0263	0.2155	0.1512
	\mathcal{G}_1	\mathcal{G}_1	0.1261	0.0263	0.1360	0.1512
Grid	$\hat{\mathcal{G}}_1$	\mathcal{G}_{crit}	0.0593	0.0224	0.0151	0.0227
	\mathcal{G}_1	\mathcal{G}_1	0.0593	0.0224	0.0151	0.0227

TABLE I

MEASURES OF DISPARITY BETWEEN THE DISCRIT GRAPH, THE EXACT DEGREE-1 GEOMETRIC GRAPH, AND THE CRITICAL GEOMETRIC GRAPH, FOR THE UNIFORM I.I.D. DEPLOYMENT, THE RANDOMISED LATTICE DEPLOYMENT, AND THE DETERMINISTIC LATTICE GRID.

IV. CGG BASED DISTANCE DISCRETISATION

In this section we show how \mathcal{G}_{crit} and DISCRIT can be useful in obtaining various optimal topologies in a distributed fashion. Given a graph, the *hop-distance*⁵ between two nodes on the graph is defined as the minimum number of hops on the graph between the nodes. We propose to use the hop-distance on \mathcal{G}_{crit} between two nodes as a measure of (Euclidean) distance between them. This technique is distributed since, we already have DISCRIT which is a distributed construction of \mathcal{G}_{crit} , and hop-distance calculation can be done using the distributed Bellman-Ford algorithm.

The concept of using hop-distance as a distance measure already exists in the literature; the important applications being DV-hop routing by Niculescu and Nath [2], and localisation by Nagpal et al. in [3]. In all these methods, the hop-distance is calculated on a specific geometric graph $\mathcal{G}(\mathbf{V}, R_0)$ where R_0 is the communication range of each node. Note that for a flat terrain and omnidirectional transmission, the edges in $\mathcal{G}(\mathbf{V}, R_0)$ join all possible direct communication neighbours. However we intend to use hop-distance on \mathcal{G}_{crit} . Our technique is advantageous over the existing methods like DV-hop in the following ways:

- 1) \mathcal{G}_{crit} is an intrinsic structure of the node layout, unlike $\mathcal{G}(\mathbf{V}, R_0)$ which is dependent on the communication parameters. Hence the proposed distance discretisation technique is independent of the communication setup.
- 2) It is shown in [3] that the error in distance estimation is proportional to the radius of the GG used for hop-distance calculation. (To see this, consider a line and if one has to express distance in integral multiples of r , then a mean error of $0.5r$ is obtained.) Thus, since r_{crit} is the smallest GG radius which ensures connectivity, using \mathcal{G}_{crit} provides better distance resolution than $\mathcal{G}(\mathbf{V}, R_0)$. Also, unlike a fixed R_0 , r_{crit} decreases with increase in n (see scaling of r_{crit} in [11]); thus the distance estimation using \mathcal{G}_{crit} keeps improving with n (also see numerical evaluation below).

Given node locations \mathbf{V} , let $h_{i,j}$ represent the hop-distance between i and j on \mathcal{G}_{crit} . Define $\rho_{i,j} = \frac{d_{i,j}}{h_{i,j}}$. Note that the proposed distance discretisation is valid if the hop-distance $h_{i,j}$ is proportional to the Euclidean distance $d_{i,j}$, i.e., if $\rho_{i,j}$ is a constant for all (i, j) pairs. Simulation results show that as n increases, $d_{i,j}$ becomes *roughly* proportional to $h_{i,j}$.

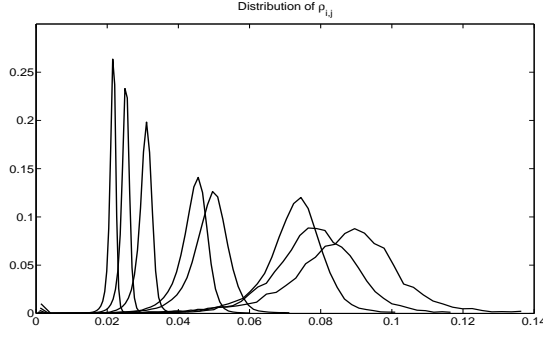


Fig. 4. Empirical distribution (normalised histogram) of $\rho_{i,j}$ for a sample uniform i. i. d. deployment for each n . 8 values of n are considered between 100 and 5000 nodes

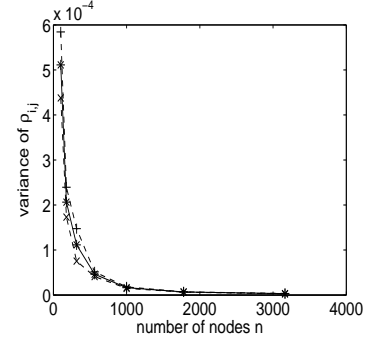


Fig. 5. Empirical variance of $\rho_{i,j}$. Confidence interval is shown for each n .

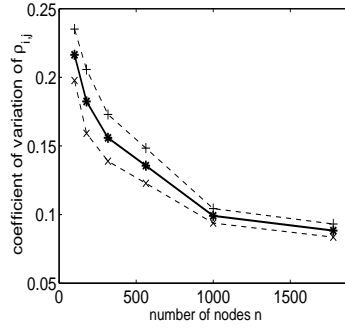


Fig. 6. Empirical coefficient of variance of $\rho_{i,j}$. Confidence interval is shown for each n .

A. Numerical Evaluation

We consider different values of n varying from 100 nodes to 5000 nodes. For each n , a sample uniform i.i.d. deployment \mathbf{V} is considered. For each \mathbf{V} , the CGG \mathcal{G}_{crit} is found, and $\rho_{i,j}$ is evaluated for every node pair (i, j) . Figure 4 shows the empirical distribution (normalised histogram) of $\rho_{i,j}$ for different n . As n is increased, the support of distribution moves to the smaller values and the distribution becomes narrower. In other words, the variation of $\rho_{i,j}$ over node pairs decreases as the node density is increased.

Figure 5 and Figure 6 show the plots of empirical variance $\sigma_{\rho}^2(\mathbf{V})$ and the empirical *coefficient of variation*⁶ $CV_{\rho}(\mathbf{V})$ of $\rho_{i,j}$ against n (along with the confidence intervals). The values of $\sigma_{\rho}^2(\mathbf{V})$ and $CV_{\rho}(\mathbf{V})$ are found to decrease as n is increased. Thus the plots indicate that the $\rho_{i,j}$ becomes *roughly* a constant for large n , thus justifying the proposed distance discretisation technique.

V. AN EXAMPLE APPLICATION: OPTIMAL SELF-ORGANISATION [8]

Here we illustrate the usefulness of \mathcal{G}_{crit} based distance discretisation (and hence of DISCRIT) to self-organisation problems involving distance information. We consider a self-organisation problem formulated in [8] of obtaining the optimal hop-length which maximises the transport capacity on a *single-cell* dense ad

⁵hop-distance is a “distance” as it satisfies the properties of non-negativity, symmetry, and triangle inequality

⁶The coefficient of variation is the ratio of standard deviation to the mean.

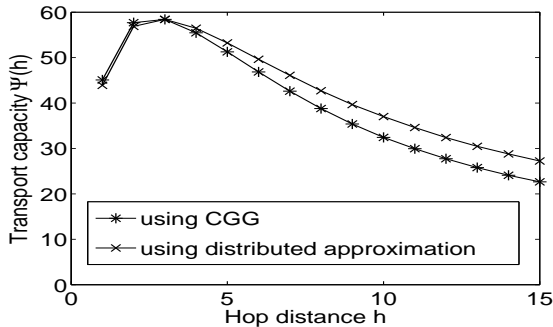


Fig. 7. Plot of Ψ_h vs. h using centralised \mathcal{G}_{crit} and $\hat{\mathcal{G}}_1$ for hop-distance calculation. The optimal hop-distance $h_{opt} = 3$ in both cases.

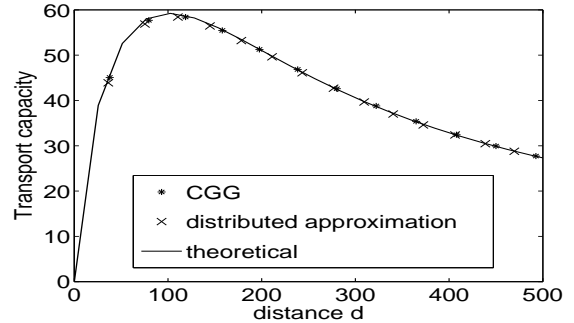


Fig. 8. Comparison of theoretical Transport capacity with those obtained from simulation. The hop-distance h is replaced by mean hop-length in T_h .

hoc network. There is a dense deployment of nodes in a limited area. Source-destination pairs are chosen randomly and the traffic is assumed to be *homogeneous*. A multihop ad hoc wireless sensor network needs to be self-organised in such a way that all communication hops are of equal length d . The multiple access protocol is such that only one successful transmission can occur at any time in the network (i.e., there is *no spatial reuse*). Although [8] considers a fading channel model, we will restrict to the no-fading case. There is a node transmit power constraint, P_t , and the nodes have the capability of achieving the Shannon capacity over the hop-length d , that is, the bit rate of $W \log \left(1 + \frac{\alpha_0 P_t}{d^\eta \sigma^2} \right)$ where W is the bandwidth and α_0 is a constant accounting for power gains between the transmitter and receiver. Under this setup, the aggregate bit rate carried by the system when all nodes transmit over a distance d per hop, takes the form (see [8]) $\lambda(d) = a \log \left(1 + \frac{\alpha_0 P_t}{d^\eta \sigma^2} \right)$ where a is a constant which depends on the contention parameters. The objective is to maximise the network *transport capacity* (in bit-meters/sec) given by

$$\Psi(d) = d\lambda(d) = a d \log \left(1 + \frac{\alpha_0 P_t}{d^\eta \sigma^2} \right) \quad (5)$$

over all hop-lengths d . It can be seen that there exists an optimal hop-distance d_{opt} which maximises $\Psi(d)$. The trade-off comes from the fact that if the network self-organises into short hop lengths, then the bit rate achieved over a hop is large, but each packet has to traverse many hops. On the other hand if d is large then the bit rate over a hop will be small, but fewer hops need to be traversed.

A. A Self-Organisation Heuristic

We aim to obtain a topology whose hop-lengths are close to d_{opt} . We employ the distance discretisation technique described in Section IV to convert the problem of finding d_{opt} to one of finding an optimal hop-distance (on \mathcal{G}_{crit}), h_{opt} , in order to maximise transport capacity. The resulting self-organisation algorithm is described below.

- 1) **Obtain the critical geometric graph \mathcal{G}_{crit} :** Given the node locations, obtain \mathcal{G}_{crit} . This is required to obtain the hop-distance information.
- 2) **Obtain h -hop-distance topology T_h :** For $h \geq 1$, the h -hop-distance topology T_h is obtained by having an edge between all node-pairs (i, j) with hop-distance $h_{i,j} = h$ on \mathcal{G}_{crit} . The edges (hops) in this topology are considered to have h units of distance. T_1 , thus, denotes the CGG.
- 3) **Find the optimal hop-distance h_{opt} :** Using each topology T_h , find the corresponding network transport capacity Ψ_h . The optimal hop-distance topology T_{opt} (equivalently the optimal hop-distance h_{opt}) is chosen to be the one which maximises Ψ_h .

B. Numerical Results

The uniform i.i.d deployment shown in Figure 2 is considered. We use both the centralised \mathcal{G}_{crit} and the distributed $\hat{\mathcal{G}}_1$ for hop-distance calculation. The hop-distances are calculated using distributed distance-vector routing, using which h -hop topologies $\{T_h\}$ are found.

Nodes are assumed to be saturated and attempt for the channel with a fixed probability. For each topology T_h , the following is done. Whenever successful, a node transmits randomly to one of its adjacent nodes in T_h , i.e., to a neighbour h hops away on \mathcal{G}_{crit} . Each node counts the number of bit-meters transmitted by it. At the end of certain time t , the network transport capacity Ψ_h is calculated as the average bit-meters transmitted by all the nodes in unit time.

The plot of transport capacity Ψ_h against the hop-distance h is shown in Figure 7. The optimal hop-distance $h_{opt} = 3$ when either of \mathcal{G}_{crit} or $\hat{\mathcal{G}}_1$ is used. We may conclude that using T_3 could be optimum for the transport capacity objective. For comparing the result from the heuristic with the theory, we plot the transport capacity Ψ_h against the *mean hop-length* in T_h , and then compare it with the theoretical plot obtained using Equation 5. The plots are shown together in Figure 8. The plots being *close* to each other verify the validity of the proposed heuristic, and the applicability of the proposed distance discretisation technique.

Thus, for the example scenario above, nodes will use T_3 as the communication topology in order to obtain a good transport capacity. That is, each node will communicate directly with nodes 3 hops away in \mathcal{G}_{crit} (or in DISCRIT output $\hat{\mathcal{G}}_1$) as $h_{opt} = 3$.

VI. APPLICATION TO NODE LOCALISATION

We illustrate another use of \mathcal{G}_{crit} and DISCRIT in estimating the locations of the nodes in a sensor network. The method described here was conceived independently by us [12], but has been also reported by Yang et al.[9], who call it *Hop Count Ratio-based Localisation* (HCRL). But the difference is that, like other existing methods which use hop-distances, HCRL also uses $\mathcal{G}(\mathbf{V}, R_0)$ (described in Section IV) for hop-distance calculation, while we use \mathcal{G}_{crit} .

A. Theory

Given the node deployment \mathbf{V} , consider n_B beacons (nodes whose positions are known) given by the set $\{B_1, B_2, \dots, B_{n_B}\}$. Let S be a node whose location is to be determined. From the distance discretisation technique described in Section IV, we take $h_{S, B_i} \propto d_{S, B_i}$ approximately for large n . Thus, for any $1 \leq i, j \leq n_b$, we have

$$\frac{d_{S, B_i}}{d_{S, B_j}} \approx \frac{h_{S, B_i}}{h_{S, B_j}} = r_{i,j} \text{ (say)} \quad (6)$$

Let (x, y) , (x_i, y_i) , and (x_j, y_j) be the co-ordinates of S , B_i , and B_j respectively. Then, taking the approximation in (6) to be an equality, we have

$$\frac{\sqrt{(x - x_i)^2 + (y - y_i)^2}}{\sqrt{(x - x_j)^2 + (y - y_j)^2}} = r_{i,j} \quad \text{solving which we get}$$

$$(1 - r_{i,j}^2) x^2 + (1 - r_{i,j}^2) y^2 - 2(x_i - r_{i,j}^2 x_j) x - 2(y_i - r_{i,j}^2 y_j) y + (x_i^2 + y_i^2) - r_{i,j}^2 (x_j^2 + y_j^2) = 0 \quad (7)$$

When $r_{i,j} = 1$, the equation above is linear and represents the perpendicular bisector of line joining B_i and B_j , whereas when $r_{i,j} \neq 1$, it represents a circle. In general, such a circle is called an *Apollonius circle* [9][13]. As we need a minimum of 3 such circles to get a point estimate of the node location, we need at

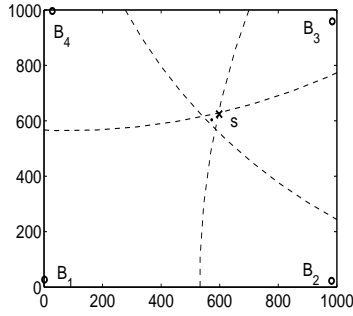


Fig. 9. Illustration of node localisation for a sample node. The actual position is shown as \times and the estimate is shown as \cdot in the figure.

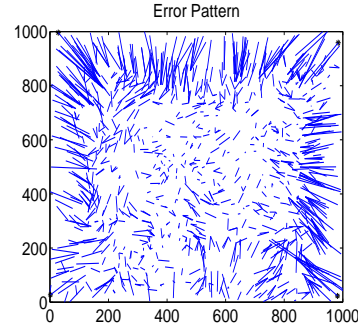


Fig. 10. Node localisation using exact \mathcal{G}_{crit} : Error pattern.

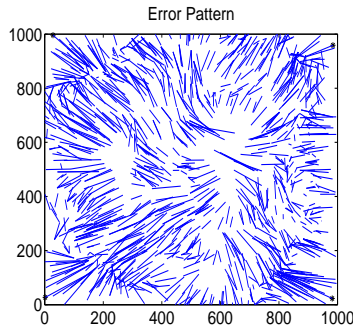


Fig. 11. Node localisation using distributed $\hat{\mathcal{G}}_1$: Error pattern.

least 4 beacons. Note that 3 Apollonius circles can be obtained even with 3 beacons, but all 3 intersect at 2 points in general, and hence an additional beacon is required.

B. Numerical Results

We consider the uniform i.i.d. deployment of 1000 nodes in a 1 Km \times 1 Km square shown in Figure 2. 4 nodes nearest to 4 corners of the square are taken as beacons (shown as \bullet in Figure 9). A sample node S is considered for the purpose of illustration (shown as \times in Figure 9). The hop-distance calculation is made on the corresponding \mathcal{G}_{crit} . 3 of the 6 possible Apollonius circles are shown in Figure 9. The circles correspond to beacon-pairs (1,2), (1,3) and (1,4). (Note that if $h_{i,j}$ were exactly proportional to $d_{i,j}$, then all the Apollonius circles would intersect at a point, which would coincide with the actual location \times .) To obtain an estimate, we use an inbuilt MATLAB function which solves an optimisation problem involving the circle equations. The estimate is shown as \cdot in Figure 9. The *error* in the position estimation, i.e., the distance between the node's actual position and the estimate is 41 m (comparable with $r_{crit}=56.7$ m).

To observe the localisation performance for all nodes, an error pattern is obtained by joining each node's actual position and its estimate. The error pattern is shown in Figure 10. The mean estimation error is 55 m. The same experiment is repeated by performing hop-distance calculation on the DISCRIT output $\hat{\mathcal{G}}_1$. The resulting error pattern is shown in Figure 11. The mean error is 74 m in this case, which is higher compared to that of centralised \mathcal{G}_{crit} . In both the cases, the error is large towards the edges because of smaller node density at the edges and since the distance discretisation technique is valid for large node densities (see

Section IV).

VII. CONCLUSION

The paper provides DISCRIT: a distributed algorithm to approximate \mathcal{G}_{crit} , using link weights obtained from the Hello-protocol-based neighbour discovery. The validity of DISCRIT is shown (with high probability) for a dense uniform i. i. d. deployment, by making use of Penrose's result and the spatial homogeneity of the deployment. Simulation results are shown for other types of deployments too, which indicate that the algorithm provides good approximations of \mathcal{G}_{crit} . Using \mathcal{G}_{crit} (and DISCRIT), a distributed technique of associating distances to links joining node pairs is also proposed. Example applications of \mathcal{G}_{crit} based distance discretisation are shown for a self-organisation problem of obtaining the optimal hop-length which maximises transport capacity for a dense ad hoc network operated as a single-cell, and also for node localisation.

In related work, we have also considered the problem of anisotropic antenna radiation patterns, which renders invalid the direct use of Hello counts as described in this paper. However, assuming that antenna patterns are randomly and uniformly oriented, nodes can locally cooperate to address the anisotropy problem.

Other extensions of this work could include handling spatially non-homogeneous deployments, which in turn will also help reduce the *edge effect* seen in DISCRIT outputs. Other practical issues to be examined are self-tuning of parameters such as the Hello transmission latency and node transmit power for improved performance of DISCRIT.

The algorithms and techniques proposed in the paper, apart from being distributed and asynchronous, require only limited capabilities from the nodes. The nodes are not equipped with position finding devices such as GPS. Receive Signal Strength (RSS) based techniques for distance estimation, which require accurate power measurement and scheduling, are also not used. Thus, our approach can provide a simple yet effective way of self-organisation in sensor networks.

REFERENCES

- [1] S. Nath and A. Kumar, "Performance evaluation of distance-hop proportionality on geometric graph models of dense sensor networks," in *Proc. Valuetools 2008*, 2008.
- [2] D. Niculescu and B. Nath, "Ad hoc positioning system," in *Proc. GLOBECOM*. IEEE, November 2001.
- [3] R. Nagpal et al., "Organizing a global coordinate system from local information on an ad hoc sensor network," in *IPSN*, 2003.
- [4] F. Ye, G. Zhong, S. Lu, and L. Zhang, "Gradient broadcast: A robust data delivery protocol for large scale sensor networks," *Wireless Networks*, vol. 11, pp. 285–298, 2005.
- [5] P. Gupta and P. R. Kumar, "The capacity of wireless networks," *IEEE Transactions on Information Theory*, March 2000.
- [6] M. D. Penrose, "On k-connectivity for a geometric random graph," *Random Structures and Algorithms archive*, September 1999.
- [7] A. Karnik and A. Kumar, "Distributed optimal self-organization in ad hoc wireless sensor networks," *IEEE Infocom*, 2004.
- [8] V. Ramaiyan, A. Kumar, and E. Altman, "Jointly optimal power control and routing for a single cell,dense,ad hoc wireless network," in *Symposium on modelling and optimization in mobile, ad hoc, and wireless networks (WiOpt)*, 2007.
- [9] S. Yang, J. Yi, and H. Cha, "HCRL: A hop-count-ratio based localization in wireless sensor networks," in *SECON*. IEEE, 2007, to appear.
- [10] S. Narayanaswamy et al., "Power control in ad-hoc networks: Theory, architecture, algorithm and implementation of the COMPOW protocol," in *European Wireless Conference*, 2002.
- [11] P. Gupta and P. R. Kumar, "Critical power for asymptotic connectivity in wireless networks," *Stochastic Analysis,Control,Optimization and Applications*, 1998.
- [12] S. Acharya, "Distributed self-organisation in dense wireless ad hoc sensor networks," Master's thesis, Indian Institute of Science, Bangalore, July 2007.
- [13] C. V. Durell, *Modern geometry: The straight line and circle*. Macmillan, 1928.

APPENDIX

APPENDIX A
PROOF OF THEOREM 2

Theorem: If \mathcal{G}_1 is connected, then the algorithm converges to \mathcal{G}_1 , i.e., $\mathcal{G}_A = \mathcal{G}_1$, in at most D iterations, where D is the *hop diameter* of \mathcal{G}_1 .

Proof: The proof proceeds in a few lemmas.

Lemma A.1: For all k , for all $i \in N$, $r^{(k)}(i) = r^{(0)}(j)$ for some $j \in N$ (j depends on i and k).

Proof: Induction on k : From **Step 3** of the algorithm, we have $r^{(k+1)}(i) = \max\{r^{(k)}(j) : j \in S^{(k)}(i)\}$. Therefore,

$$r^{(k)}(i) = r^{(k-1)}(i_1) = \dots = r^{(1)}(i_{k-1}) = r^{(0)}(j)$$

for some $i_1, i_2, \dots, j \in N$. ■

Lemma A.2: For all $i \in N$, for all k , $r^{(k)}(i) \leq r_1$.

Proof: From Lemma A.1, $r^{(k)}(i) = r^{(0)}(j)$ for some $j \in N$. Therefore

$$r^{(k)}(i) = r^{(0)}(j) = \min_{k \in N, k \neq j} \{d_{j,k}\} \leq \max_{j \in N} \{ \min_{k \in N, k \neq j} \{d_{j,k}\} \} = r_1$$

Lemma A.3: If $r^{(k)}(i) = r_1$ for some k , then for $s = 1, 2, 3, \dots$, $r^{(k+s)}(i) = r_1$

Proof: Note that $i \in N^{(k)}(i)$ since $d_{i,i} = 0$, and hence $i \in S^{(k)}(i)$. Thus

$$r^{(k+1)}(i) = \max\{r^{(k)}(j) : j \in S^{(k)}(i)\} \geq r^{(k)}(i) = r_1$$

But from Lemma A.2, $r^{(k+1)}(i) \leq r_1$, therefore $r^{(k+1)}(i) = r_1$.

The argument can be extended to show $r^{(k+s)}(i) = r_1$ for $s = 2, 3, \dots$ ■

Let $l = \arg \max_{i \in N} \{r^{(0)}(i)\}$. Then, $r^{(0)}(l) = r_1$. Let $C(h) = \{i : i \text{ is connected to } l \text{ in } h \text{ hops in } \mathcal{G}_1\}$.

Lemma A.4: For all $i \in C(h)$, $r^{(h)}(i) = r_1$.

Proof: Induction on h : $i \in C(1)$ means that $d_{i,l} \leq r_1 = r^{(0)}(l)$. Therefore, $i \in N^0(l) \Rightarrow l \in S^{(0)}(i)$, and hence, $r^{(1)}(i) \geq r^{(0)}(l) = r_1$. But from Lemma A.2, $r^{(1)}(i) \leq r_1$. Therefore, $r^{(1)}(i) = r_1$.

Assume, for all $i \in C(h)$, $r^{(h)}(i) = r_1$. Now, for any $i \in C(h+1)$, there exists a $j \in C(h)$ such that $d_{i,j} \leq r_1$. Thus $r^{(h)}(j) = r_1 \Rightarrow i \in N^{(h)}(j)$, and hence $j \in S^{(h)}(i)$. Therefore $r^{(h+1)}(i) = \max\{r^{(h)}(t) : t \in S^{(h)}(i)\} \geq r^{(h)}(j) = r_1$. Again from Lemma A.2, $r^{(h+1)}(i) = r_1$ for all $i \in C(h+1)$.

Lemma A.4 now follows from the induction principle. ■

Lemma A.5: Suppose \mathcal{G}_1 is *connected*. Let m be the maximum number of hops in the least-hop path on \mathcal{G}_1 between any node i and l (m is the *hop radius* of \mathcal{G}_1 centered at l). Then the algorithm converges in m iterations. Moreover $r(i) = r_1$ for all i .

Proof: Take any node $i \in N$. Since \mathcal{G}_1 is connected, $i \in C(h)$ for some $h \leq m$. Now from Lemma A.4, $r^{(h)}(i) = r_1$ and therefore from Lemma A.3, $r^{(m)}(i) = r_1$ as $m \geq h$.

Now at m^{th} iteration, we have $r^{(m)}(i) = r_1$ for all $i \in N$. Therefore from Lemma A.2, $r^{(m+1)}(i) = r_1$ for all i .

Thus at **Step 4**, the algorithm terminates and $r(i) = r_1$ for all $i \in N$. ■

Thus, from Lemma A.5, $r(i) = r_1$, and $N(i) = \{j : d_{i,j} \leq r_1\}$. Now from **Step 5** of the algorithm, it can be seen that $\mathcal{G}_A = \mathcal{G}_1$. Theorem 2 follows by observing the fact that $m \leq D$, the hop diameter of \mathcal{G}_1 . ■

APPENDIX B PROOF OF THEOREM 3

Theorem: For any $\epsilon > 0$ however small,

$$\lim_{n \rightarrow \infty} \mathcal{P}^n \left\{ \mathbf{V} : \frac{n}{|\mathcal{A}|} (1 - \epsilon) \leq \frac{N_r(x; \mathbf{V})}{\pi r^2} \leq \frac{n}{|\mathcal{A}|} (1 + \epsilon) \text{ for every } x \in \tilde{\mathcal{A}}(r) \right\} = 1$$

Proof: Note that the expression contained within $\mathcal{P}^n\{\cdot\}$ involves an intersection of (uncountably) infinite events, where each event corresponds to a bound on $N_r(x; \mathbf{V})$ for each point $x \in \tilde{\mathcal{A}}(r)$. For this purpose, we make use of uniform convergence of weak law of large numbers, given by *Vapnik-Chervonenkis* theorem.

Given a set U , let \mathcal{C} be a collection of subsets of U . Let F be a finite subset of U . F is said to be *shattered* by \mathcal{C} if for every subset G of F , there exists a subset $C \in \mathcal{C}$ such that $F \cap C = G$. The *VC-dimension* of \mathcal{C} is defined as the supremum of sizes of all finite sets (F s) that can be shattered by \mathcal{C} .

Theorem 4 (Vapnik and Chervonenkis): If \mathcal{C} is a set of finite VC-dimension $d_{\mathcal{C}}$, and $\{X_i\}_{i=1}^m$ be a sequence of i.i.d random variables taking values in U with common probability distribution P , then for every $\epsilon', \delta > 0$

$$\Pr \left(\sup_{C \in \mathcal{C}} \left| \frac{\sum_{i=1}^m I_{\{X_i \in C\}}}{m} - P(C) \right| \leq \epsilon' \right) \geq 1 - \delta$$

whenever

$$m \geq \max \left\{ \frac{d_{\mathcal{C}}}{\epsilon'} \log \frac{16e}{\epsilon'}, \frac{4}{\epsilon'} \log \frac{2}{\delta} \right\}$$

■

Here $I_{\{\cdot\}}$ represents the indicator function. For our purpose, let U represent \mathbf{R}^2 . Then F represents a finite set of points in \mathbf{R}^2 . Define a *closed disc* of radius $r > 0$ and centre x as $D_r(x) := \{y \in \mathbf{R}^2 : \|x - y\| \leq r\}$. Let \mathcal{C} represent a collection of all closed discs in \mathbf{R}^2 , i.e., $\mathcal{C} := \{D_r(x) : x \in \mathbf{R}^2, r > 0\}$. Gupta and Kumar in [5] have shown the following.

Lemma 6: The VC-dimension of set of all closed discs in \mathbf{R}^2 is 3, i.e., $d_{\mathcal{C}} = 3$. ■

By definition $D_r(x) \in \mathcal{C}$ for every $x \in \tilde{\mathcal{A}}(r)$. Now if we take the common probability distribution P in Theorem 4 to be the uniform measure \mathcal{P} on \mathcal{A} , then it can be seen that i.i.d. random variable sequence $\{X_i\}$ is nothing but a uniform i.i.d. deployment \mathbf{V} on \mathcal{A} . Now observing that $\mathcal{P}\{D_r(x)\} = \frac{\pi r^2}{|\mathcal{A}|}$ for all $x \in \tilde{\mathcal{A}}(r)$, Theorem 4 and Lemma 6 give rise to the following result.

Corollary 2: For every $\epsilon', \delta > 0$

$$\mathcal{P}^n \left\{ \left| \frac{\sum_{i=1}^n I_{\{V_i \in D_r(x)\}}}{n} - \frac{\pi r^2}{|\mathcal{A}|} \right| \leq \epsilon' \quad \text{for every } x \in \tilde{\mathcal{A}}(r) \right\} \geq 1 - \delta$$

whenever $n \geq \max \left\{ \frac{3}{\epsilon'} \log \frac{16e}{\epsilon'}, \frac{4}{\epsilon'} \log \frac{2}{\delta} \right\}$

■

Now
$$\left| \frac{\sum_{i=1}^n I_{\{V_i \in D_r(x)\}}}{n} - \frac{\pi r^2}{|\mathcal{A}|} \right| \leq \epsilon' \Leftrightarrow n \left(\frac{\pi r^2}{|\mathcal{A}|} - \epsilon' \right) \leq \sum_{i=1}^n I_{\{V_i \in D_r(x)\}} \leq n \left(\frac{\pi r^2}{|\mathcal{A}|} + \epsilon' \right)$$

$$\Leftrightarrow \frac{n}{|\mathcal{A}|} \left(1 - \frac{|\mathcal{A}| \epsilon'}{\pi r^2} \right) \leq \frac{\sum_{i=1}^n I_{\{V_i \in D_r(x)\}}}{\pi r^2} \leq \frac{n}{|\mathcal{A}|} \left(1 + \frac{|\mathcal{A}| \epsilon'}{\pi r^2} \right)$$

Thus Corollary 2 becomes

For every $\epsilon', \delta > 0$

$$\mathcal{P}^n \left\{ \frac{n}{|\mathcal{A}|} \left(1 - \frac{|\mathcal{A}| \epsilon'}{\pi r^2} \right) \leq \frac{\sum_{i=1}^n I_{\{V_i \in D_r(x)\}}}{\pi r^2} \leq \frac{n}{|\mathcal{A}|} \left(1 + \frac{|\mathcal{A}| \epsilon'}{\pi r^2} \right) \quad \text{for every } x \in \tilde{\mathcal{A}}(r) \right\} \geq 1 - \delta$$

whenever $n \geq \max \left\{ \frac{3}{\epsilon'} \log \frac{16e}{\epsilon'}, \frac{4}{\epsilon'} \log \frac{2}{\delta} \right\}$

Theorem 3 now follows by taking $\epsilon := \frac{|\mathcal{A}| \epsilon'}{\pi r^2}$, and observing that $N_r(x; \mathbf{V}) = \sum_{i=1}^n I_{\{V_i \in D_r(x)\}}$, the number of nodes in $D_r(x)$. ■